microRNA-301a regulation of a T-helper 17 immune response controls autoimmune demyelination

Marcin P. Mycko, Maria Cichalewska, Agnieszka Machlanska, Hanna Cwiklinska, Magdalena Mariasiewicz, and Krzysztof W. Selmaj[1]

Laboratory of Neuroimmunology, Department of Neurology, Medical University of Lodz, 90-153, Lodz, Poland

Edited by Vijay K. Kuchroo, Brigham and Women's Hospital and Harvard Medical School, Boston, MA, and accepted by the Editorial Board March 19, 2012 (received for review October 5, 2011)

MicroRNAs (miRNAs) are an emerging group of short, noncoding RNAs that play an important role in regulating expression of classical genes. Thus far little is known about their role in autoimmune demyelination. In this study, we analyzed changes in the miRNA profile in $CD4^+$ T cells that occurred during the recognition of the myelin autoantigen, $MOG_{35–55}$. We found that, both in vivo and in vitro, myelin antigen stimulation resulted in significant up-regulation of miR-301a, miR-21, and miR-155. Furthermore, these three miRNAs were overexpressed in T cells infiltrating the CNS in animals with experimental autoimmune encephalomyelitis. Use of specific miRNA antagonists, antagomirs, revealed that miR-301a contributed to the development of the T-helper type 17 subset via targeting the IL-6/23–STAT3 pathway. This contribution appeared to be mediated by the miR-301a effect on the expression of the PIAS3, a potent inhibitor of the STAT3 pathway. Manipulation of miR-301a levels or PIAS3 expression in myelin-specific $CD4^+$ T cells led to significant changes in the severity of experimental autoimmune encephalomyelitis. Thus, we have identified a role of miR-301a in regulating the function of myelin-reactive T-helper type 17 cells, supporting a role for miR-301a and PIAS3 as candidates for therapeutic targets for controlling of autoimmune demyelination.

Multiple sclerosis (MS) is an organ-specific autoimmune disease manifested by chronic inflammatory demyelination of the CNS. $CD4^+$ T-cell–mediated autoimmunity, with a critical role of a putative myelin autoantigen, has long been accepted as one of the most important aspects of MS pathogenesis, especially for the early initiation of disease (1). This understanding has been particularly complemented by the research on the MS animal model, experimental autoimmune encephalomyelitis (EAE). T-helper type 1 (Th1) cells, characterized by the expression of the transcription factor T-bet and the production of IFN-γ, originally were considered the major effector T-helper cells that mediate the pathogenesis of autoimmune demyelination (2). More recently another subset of T-helper cells, Th17, characterized by expression of the transcription factors retinoic acid receptor-related orphan receptor alpha (ROR-α) and retinoic acid receptor-related orphan receptor gamma t (ROR-γt) and by the production of IL-17, has been considered pivotal for the propagation of autoimmune demyelination (3). Mice with impaired numbers or function of Th17 cells, particularly mice deficient in the cytokines IL-6 or IL-23, are largely resistant to EAE (4–6). However, precise mechanisms governing the development and function of Th17 cells resulting in autoimmune demyelination are still unclear. Thus, Th17-targeting therapeutic approaches for MS have not yet been established.

MicroRNAs (miRNAs) have begun to emerge as an important component in the differentiation and function of cells involved in the immune response. miRNAs operate as noncoding RNA molecules ~22 nt in length that are processed from larger transcripts of nonclassical genes by Drosha and Dicer nucleases (7). miRNAs are incorporated along with core argonaute proteins into the RNA-induced silencing complex. Binding of this complex to the products of classical genes in mammalian cells leads to direct or indirect interference, thus resulting in lower protein expression (8). It has been estimated that expression of as many as one-third of the classical genes may be regulated by miRNA (9). Recently, emerging data have documented the importance of miRNA in EAE development. miR-326 (10) and miR-155 (11) modulate T-cell and dendritic cell function, whereas miR-124 (12) controls quiescence of the CNS-resident antigen-presenting cell (APC) population, microglia. Furthermore, ways of blocking microRNA activity in vivo have been pursued. The best validated is the use of chemically engineered oligonucleotides, termed "antagomirs," that act as efficient, specific, and safe silencers of endogenous miRNAs in vivo and in vitro (13, 14). Thus, microRNA-targeted therapies have become an option for treatment of autoimmune demyelination.

To extend our knowledge of the role of miRNA in autoimmune demyelination and to define potential goals for miRNA-targeted therapies, we screened for changes in miRNAs in $CD4^+$ T cells during myelin antigen recognition in vitro and in vivo. Here we report that miR-301a, miR-21, and miR-155 are up-regulated significantly in T-helper cells in response to myelin oligodendrocyte protein (MOG) antigen. In a series of experiments, we identified a role for miR-301a in regulating Th17 differentiation and its in vivo contribution to the pathogenesis of autoimmune demyelination. We found that the effect of miR-301a on Th17 cells was mediated by the inhibition of PIAS3, a negative regulator of the STAT3 activation pathway.

Results

miR-21, miR-155, and miR-301a Are Up-Regulated in T-Helper Cells During the Response to the Myelin Autoantigen. To identify the changes in miRNA levels during the development of the response to myelin autoantigen in vivo, we immunized C57BL/6 mice with MOG peptide 35–55 ($MOG_{35–55}$) in Freund's complete adjuvant (CFA). Fourteen days later inguinal and popliteal peripheral lymph node (PLN) cells of $MOG_{35–55}$/CFA-immunized and control mice were stimulated in vitro with $MOG_{35–55}$. Subsequently, $CD4^+$ T cells were purified and used as a source of RNA for the microarray analysis of the miRNA expression. The results of miRNA expression profiling highlighted an up-regulation in the expression of three distinct miRNA—miR-21, miR-155, and miR-301a—in the $CD4^+$ T cells of $MOG_{35–55}$/CFA-immunized mice when restimulated with $MOG_{35–55}$ (Fig. 1*A*). To confirm the significance of the observed changes in the miRNA profiling, we analyzed extensively the relative expression levels of miR-21, miR-155, and miR-301a in PLN of the $MOG_{35–55}$/CFA-immunized mice and naive mice. Indeed, we saw a significant up-regulation of the expression of all three miRNA in $MOG_{35–55}$-

Author contributions: M.P.M. and K.W.S. designed research; M.P.M., M.C., A.M., H.C., and M.M. performed research; M.P.M. and K.W.S. analyzed data; and M.P.M. and K.W.S. wrote the paper.

The authors declare no conflict of interest.

This article is a PNAS Direct Submission. V.K.K. is a guest editor invited by the Editorial Board.

Data deposition: The microRNA expression array data reported in this paper have been deposited in the Gene Expression Omnibus database (GEO), http://www.ncbi.nlm.nih.gov/geo/ (accession no. GSE28473).

[1]To whom correspondence should be addressed. E-mail: kselmaj@afazja.am.lodz.pl.

See Author Summary on page 7600 (volume 109, number 20).

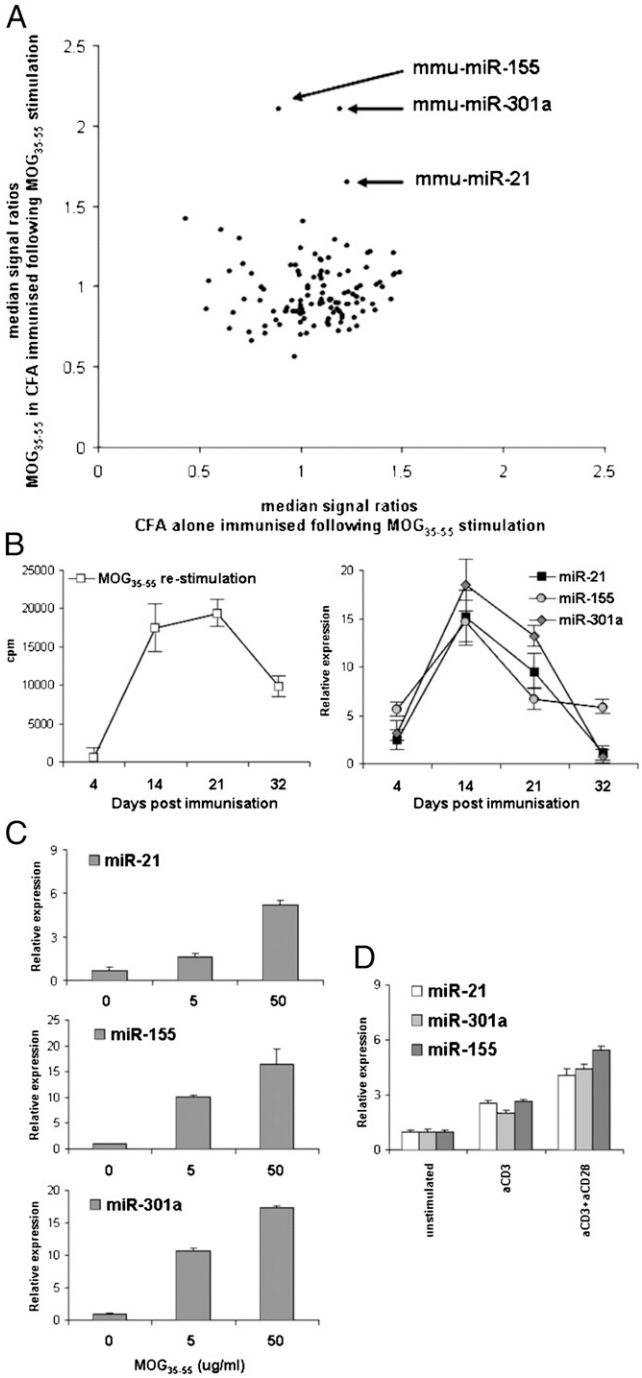

Fig. 1. Quantitative analysis of miRNA changes in CD4$^+$ T cells responding to myelin antigen. (*A*) Mice were immunized with $MOG_{35–55}$ in CFA or with CFA alone, and 14 d later PLN cells were isolated and stimulated in vitro with $MOG_{35–55}$ for 3 d followed by CD4$^+$ T-cell sorting. Microarray analysis of miRNA expression profiles was performed comparing sorted CD4$^+$ T cells from mice immunized with $MOG_{35–55}$ in CFA with CD4$^+$ T cells from mice immunized with CFA alone. miR-21, miR-155, and miR-301a showed highest expression levels after $MOG_{35–55}$ stimulation. Data represent a plot of the median of ratios of the miRNA probe signal from the individual sample versus the miRNA probe signal for pooled samples (n = 5 mice per group). (*B*) Kinetics of the response of PLN cells from $MOG_{35–55}$-immunized mice following 3-d restimulation in vitro to $MOG_{35–55}$ proliferation (*Left*) and changes in expression levels of miR-21, miR-155, and miR-301a (*Right*), normalized to day 0 responses. Data represent mean ± SEM of two or three mice per time point. (*C*) Analysis of expression of miR-21, miR-155, and miR-301a in CD4$^+$ T cells from PLNs of 2D2 mice stimulated in vitro with different doses of $MOG_{35–55}$. Representative results (mean ± SEM) from three independent experiments are shown. (*D*) Analysis of expression of miR-21, miR-155, and miR-301a in naive CD4$^+$ T cells from PLNs of C57BL/6 mice stimulated with plate-bound anti-CD3 or with plate-bound anti-CD3 and anti-CD28. Representative results (mean ± SEM) from three independent experiments are shown.

restimulated CD4$^+$ T cells as early as day 4 after immunization (Fig. 1*B*). Expression levels for all the analyzed miRNAs reached a maximum around day 14 after antigen challenge, followed by a decline to the initial response levels by day 32. The kinetics of miR-21, miR-155, and miR-301a expression responses in CD4$^+$ T cells following $MOG_{35–55}$/CFA immunization resembled the changes in the proliferative responses of PLN induced by $MOG_{35–55}$ restimulation, with miR-301a showing the highest up-regulation (Fig. 1*B*). Furthermore, we analyzed the changes in expression in the CD4$^+$ T cells of mice that transgenically express T-cell receptor alpha (TCRα) and TCRβ chains of a $MOG_{35–55}$-reactive T-cell clone (15). $MOG_{35–55}$–TCR CD4$^+$ (henceforth, "2D2") T cells displayed a strong up-regulation of miR-21, miR-155, and miR-301a expression in response to increasing doses of $MOG_{35–55}$ antigen (Fig. 1*C*). We also detected an up-regulation of miR-21, miR-155, and miR-301a expression in naive CD4$^+$ T-cells in response to anti-CD3 and anti-CD3/CD28 stimulation (Fig. 1*D*), although this up-regulation was less robust than the response following antigenic peptide recognition. Collectively our data indicate that miR-21, miR-155, and miR-301a are particularly up-regulated in response to in vitro TCR stimulation of CD4$^+$ T cells.

miR-301a Is Overexpressed by Infiltrating T Cells in the CNS of Animals with EAE. To explore the in vivo significance of miRNA changes observed following in vitro TCR restimulation, we analyzed miR-21, miR-155, and miR-301a expression in animals sensitized to develop EAE. We isolated the mononuclear cells from the brains (BMN) of animals at different stages of the disease, from day 0 (control), day 12 (preclinical), day 27 (acute EAE), and day 60 (EAE remission). As expected, the flow cytometry profiles of the BMN cells confirmed significant increases in T cells during the course of EAE (Fig. 2*A*). These inflammatory changes were accompanied by a several-fold up-regulation of miR-21, miR-155, and miR-301a expression (Fig. 2*B*). The presence of all three microRNAs increased during the acute phase of the disease (up to day 27). miR-21 and miR-155 continued to be highly overexpressed during the late stage of EAE (day 60), whereas mir-301a expression declined during the remission period (Fig. 2*B*). Thus, miR-301a overexpression within the infiltrating cells may reflect a role that differs from that of miR-21 and miR-155.

EAE inflammatory BMN cells can be divided into several distinct populations: T cells, microglia, and active APCs (macrophages and activated microglia). To identify which population was responsible for the observed miRNA overexpression, high-purity sorted fractions of each cell population were analyzed for miR-21, miR-155, and miR-301a expression during two different phases of EAE: acute (day 27) and remission (day 60) (Fig. 2*C*). The greatest changes in miR-21 and miR-155 expression occurred in the brain T-cell fraction and in macrophages and activated microglia (CD11b$^+$CD45^{hi}), with essentially no changes in the classical microglia (CD11b$^+$CD45^{int}). Changes in miR-301a expression were associated almost exclusively with the brain T-cell fraction, most notably during the acute disease phase (Fig. 2*C*). These in vivo data support a specific up-regulation of miR-301a in T cells during acute EAE.

miR-301a Inhibition Down-Regulates Th17 Responses. To search for a role for miR-21, miR-155, and miR-301a in activated T cells, we applied selective miRNA antagonists, antagomirs. None of the antagomirs affected the proliferative responses of T cells, regardless of whether the response was induced specifically by antigen or by a nonantigen (Fig. 3 *A* and *B*). However, miRNA

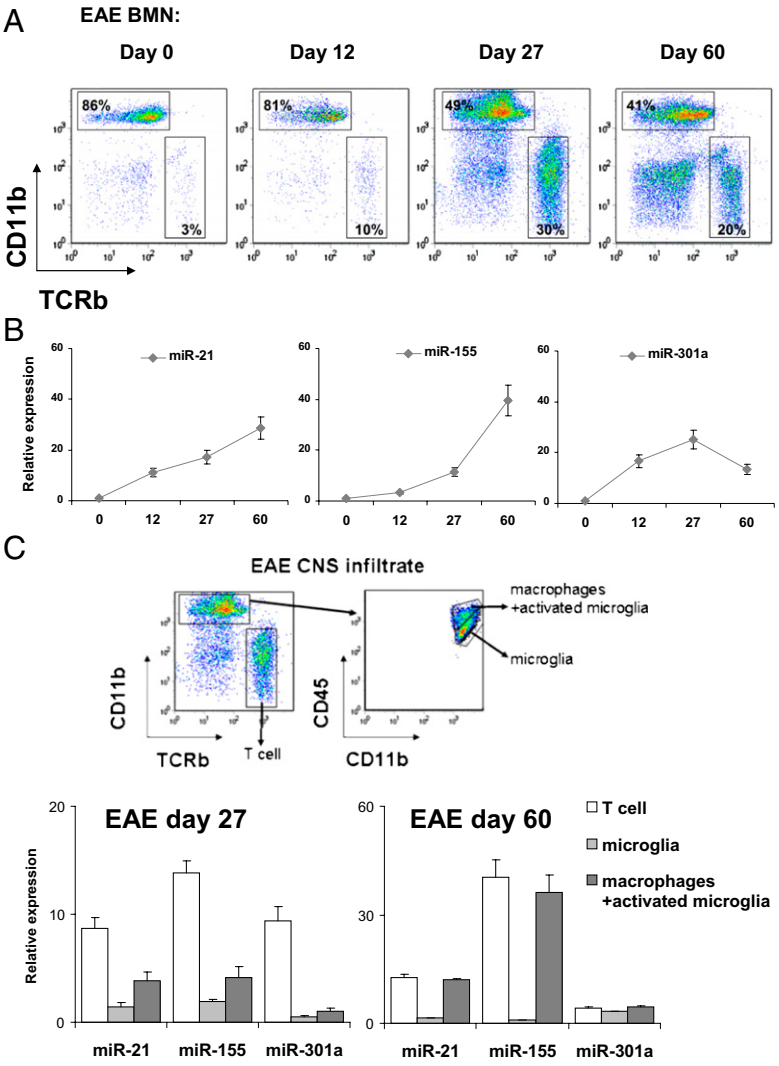

Fig. 2. Analysis of expression of miR-21, miR-155, and miR-301a in the CNS during EAE. (*A*) BMN composition in naive mice (day 0) or mice at the preclinical (day 12), peak (day 27), or remission (day 60) stage of EAE. Four or five mice per group were used. (*B*) Kinetics of expression of miR-21, miR-155, and miR-301a in EAE BMN at different days after disease induction as shown by qPCR. Representative results (mean ± SEM) from two or three independent experiments are shown. Four or five brains were used in each experiment. (*C*) BMN from mice at the peak (day 27) or remission (day 60) stage of EAE were sorted by flow cytometry into T-cell ($TCR\beta^+CD11b^-$), microglia ($CD11b^+CD45^{int}$), and macrophages/activated microglia ($CD11b^+CD45^{hi}$) subsets. Subsequently these fractions were analyzed for levels of miR-21, miR-155, and miR-301a by qPCR, normalized to BMN expression in naive mice. Representative results (mean ± SEM) from two independent experiments are shown. Four or five brains were used in each experiment.

blockade resulted in significant changes in the cytokine secretion profiles following $MOG_{35–55}$ stimulation (Fig. 3 *C–F*). Antagomirs against miR-21 and miR-155 resulted in down-regulation of IFN-γ secretion and a minor up-regulation of IL-4 secretion. However, most notably, transfection with antagomir against miR-301a resulted in decreased IL-17 secretion, whereas antagomirs against miR-21 and miR-155 had no significant effect on this cytokine (Fig. 3*D*). In addition, an antagomir against miR-301a resulted in increased IL-4 production (Fig. 3*E*). IL-10 production levels were largely unaffected by any of the three antagomirs (Fig. 3*F*). These data suggest miR-301a has a strong influence on the Th17-like cytokine secretion profile.

To confirm the effects of miR-21, miR-155, and miR-301a on T-helper cell profiles, we subsequently analyzed the expression pattern of gene markers of T-helper cell differentiation (Fig. 3*G*). In highly purified $CD4^+$ T cells fluorescently labeled with antagomirs, we found that inhibition of miR-155 led to an increase in *Gata3* expression reminiscent of a Th2 shift described in miR-155-deficient mice (16). The levels of transcription for *Tbx21* and *Foxp3* were largely unaffected by the inhibition of any of the studied miRNAs. Most notably, the antagomir against miR-301a treatment resulted in a marked decrease in mRNA for *Rora*, *Rorc-γt*, *Ahr*, *Il17A*, and *Il17F*, indicating a strong influence on Th17 differentiation (Fig. 3*G*). These data suggest that miR-301a is specifically involved in Th17 cell differentiation but not in Th1 cell differentiation.

In Vitro Modulation of miR-301a in T Cells Impacts Th17 Differentiation. To confirm further the relationship between miR-301a and Th17 cells, we compared the expression levels of this miRNA in different T-helper cell subsets: Th1, Th2, Th17, and naive T-helper cells. We found that ex vivo Th17 cells expressed miR-301a at very high levels in comparison with the other T-helper cell subsets (Fig. 4*A*).

In addition, we analyzed the kinetics of miR-301a expression during the in vitro differentiation of Th17 cells. We observed a highly significant up-regulation of miR-301a in the Th17-polarized naive T cells as early as 3 d after the start of differentiation (Fig. 4*B*). When we analyzed the miR-301a expression profiles of the various in vitro-generated T-helper cell populations, miR-301a was enriched most significantly in the Th17 subset (Fig. 4*C*). Furthermore, we assessed the effect of miR-301a inhibition on the in vitro development of Th17 cells. We found that inhibition of miR-301a in naive $CD4^+$ T cells rendered them fourfold less sufficient for in vitro generation of Th17 cells (Fig. 4*D*). In addition, we observed that expression of CCR6, a chemokine receptor linked to a Th17-cell phenotype (17), was down-regulated in stimulated naive $CD4^+$ T cells when miR-301a was blocked by antagomir and, conversely, was up-regulated by an miR-301a mimic (Fig. 4*E*). Thus, these data strongly suggested that miR-301a promotes differentiation of the Th17 subset.

miR-301a Interferes with the IL-6–STAT3 Phosphorylation Pathway. Because different signaling pathways [e.g., TGF-β, IL-6, and IL-23 (3, 5, 18)] contribute to Th17 generation in vitro, we in-

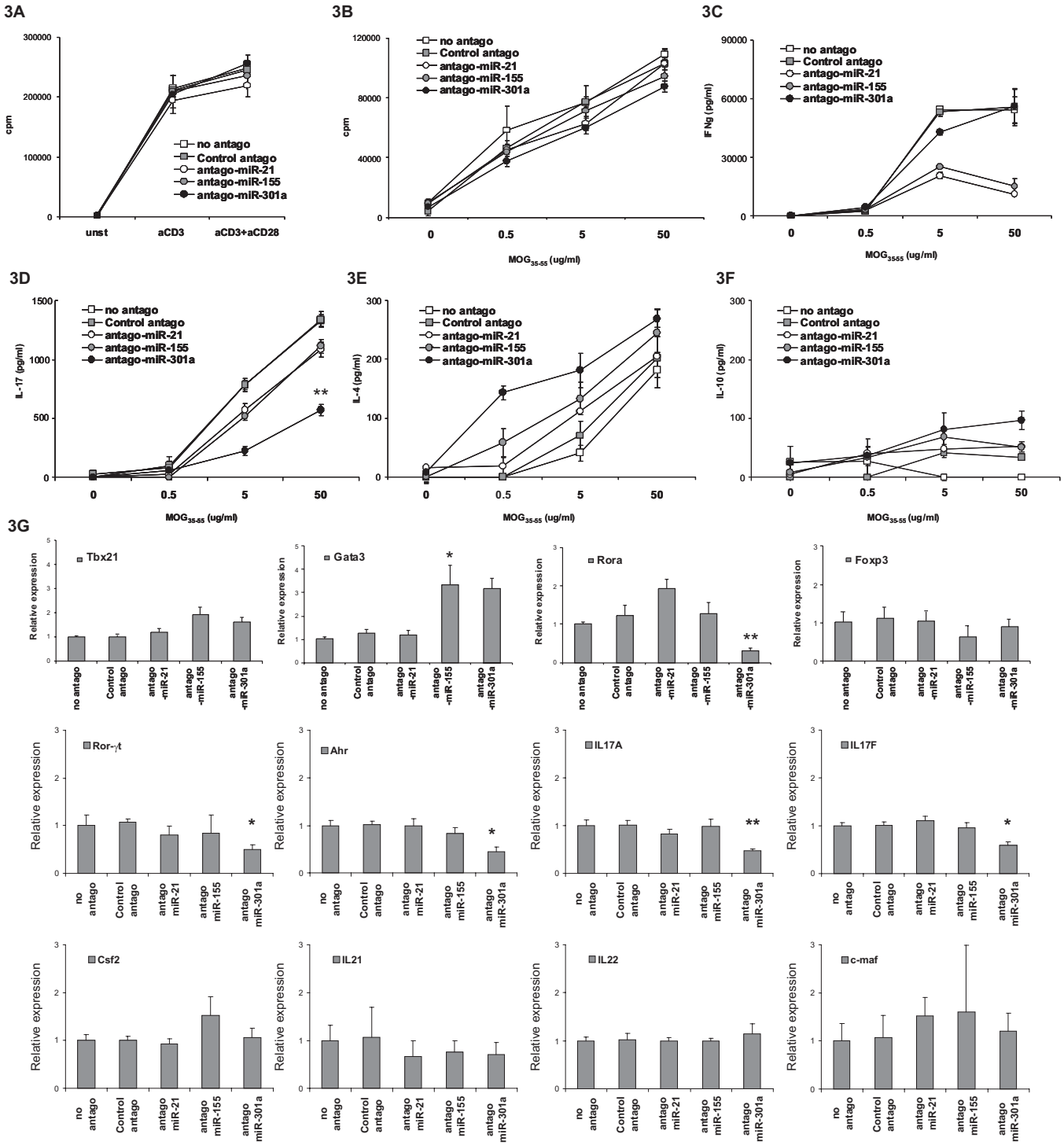

Fig. 3. Effects of antagomir inhibition of miR-21, miR-155, and miR-301a on CD4$^+$ T-cell function. (*A*) PLN CD4$^+$ T cells were transfected with antagomirs against miR-21, miR-155, miR-301a, or control antagomir, and their proliferative responses to plate-bound anti-CD3 or plate-bound anti-CD3 and anti-CD28 stimulation were compared with the responses of untransfected PLN CD4$^+$ T cells. Representative results (mean ± SEM) from three independent experiments are shown. (*B*) PLN cells of mice immunized 12 d earlier with $MOG_{35–55}$ were transfected with antagomirs against miR-21, miR-155, miR-301a, or control antagomir or were not transfected following in vitro restimulation for 3 d with indicated doses of $MOG_{35–55}$. Proliferative responses were analyzed. (*C–F*) Culture supernatants were analyzed for the levels of IFN-γ (*C*), IL-17 (*D*), IL-4 (*E*), and IL-10 (*F*). Representative results (mean ± SEM) from three independent experiments are shown. $^{**}P < 0.001$. (*G*) PLN cell cultures, as described in *B*, were restimulated in vitro with 50 μg/mL of $MOG_{35–55}$. Subsequently antagomir-affected CD4$^+$ T cells were sorted, and RNA was analyzed with qPCR for expression levels of *Tbx21*, *Gata3*, *Rora*, *Foxp3*, *Ror-γt*, *Ahr*, *Il17A*, *Il17F*, *CSf2*, *Il21*, *Il22*, and *c-maf*. Data were normalized to the expression levels in CD4$^+$ T cells from untransfected cultures. Representative results (mean ± SEM) from three independent experiments are shown. $^{*}P < 0.05$, $^{**}P < 0.001$.

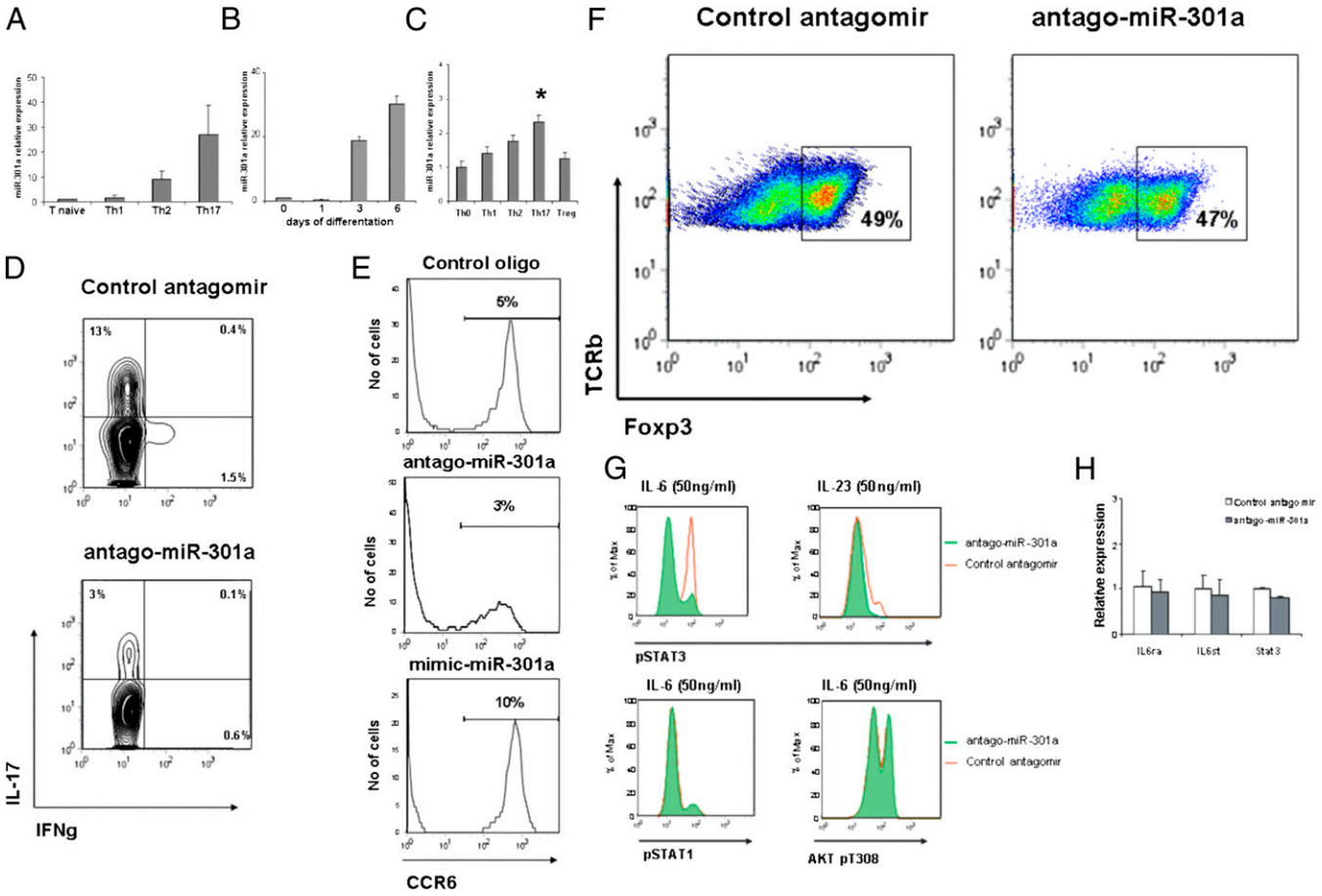

Fig. 4. Analysis of the role of miR-301 in T-helper cell differentiation. (*A*) RNA was extracted from ex vivo sorted Th1, Th2, and Th17 cells and analyzed for the expression levels of miR-301a by qPCR. The miR-301a expression data were normalized for the expression of U6 snRNA and were compared with the expression level of naive CD4$^+$ T cells. Representative results (mean ± SEM) from two to four independent experiments are shown. (*B*) Naive CD4$^+$ T cells were stimulated in vitro with plate-bound anti-CD3 and anti-CD28 in the presence of IL-6, TGF-β, IL-1β, IL-23, anti–IFN-γ, and anti–IL-4 to polarize them toward Th17 cells. RNA was extracted at the indicated days, and miR-301a levels were assessed by qPCR and compared with the day 0 levels. Representative results (mean ± SEM) from two independent experiments are shown. (*C*) Naive CD4$^+$ T cells were stimulated in vitro with plate-bound anti-CD3 and anti-CD28, in the Th0-, Th1-, Th2-, Th17-, and Treg-polarizing condition. RNA was extracted at the day 14, and miR-301a levels were assessed by qPCR and compared with the expression level of the Th0 condition. Representative results (mean ± SEM) from two independent experiments are shown. *$P < 0.01$ (*D*) Naive CD4$^+$ T cells were transfected with an antagomir against miR-301a or with a control antagomir, were polarized toward Th17 cells as described in *B*, and were assayed for the secretion of IL-17 and IFN-γ by intracellular flow cytometry on day 6 after the start of stimulation. The data show gated antagomir-positive cells. Representative results from four independent experiments are shown. (*E*) Naive CD4$^+$ T cells were transfected with an antagomir against miR-301a or with a mimic for miR-301a or with a control oligonucleotide, were stimulated for 3 d with plate-bound anti-CD3 and anti-CD28, and were assayed for surface expression of CCR6 by flow cytometry. The data show gated antagomir-positive cells. Representative results from four independent experiments are shown. (*F*) Naive CD4$^+$ T cells were transfected with antagomir against miR-301a (antago-miR-130a) or with a control antagomir and were stimulated in vitro with plate-bound anti-CD3 and anti-CD28 in the presence of TGF-β, IL-2, anti–IFN-γ, and anti–IL-4 to polarize them toward Treg cells. Cells were assayed for the presence of FOXP3 by intracellular flow cytometry on day 6 after the start of stimulation. The data show gated antagomir-positive cells. Representative results from two independent experiments are shown. (*G*) CD4$^+$ T cells were transfected with antagomir against miR-301a or with a control antagomir, were stimulated in vitro with either IL-6 or IL-23 for 30 min at 37 °C, and were assayed for pSTAT3 by intracellular flow cytometry (*Upper*) or were stimulated in vitro with IL-6 for 30 min at 37 °C and were assayed for pSTAT1 (*Lower Left*) or for pAKT (*Lower Right*) by intracellular flow cytometry. The data show gated antagomir-positive cells. Representative results from two to four independent experiments are shown. (*H*) CD4$^+$ T cells were transfected with antagomir against miR-301a or with a control antagomir and were stimulated in vitro with plate-bound anti-CD3 and anti-CD28 for 3 d. Antagomir-positive cells were sorted by flow cytometry, and RNA was isolated and analyzed for the expression levels of *IL6ra*, *IL6st*, and *Stat3* by qPCR. Data were normalized to the expression levels of unstimulated CD4$^+$ T cells. Representative results (mean ± SEM) from three independent experiments are shown.

vestigated which pathways might be affected by miR-301a. For the TGF-β pathway, we analyzed in vitro differentiation of naive T cells into regulatory T-cells (Tregs) in the presence of antagomir for miR-301a and found no changes in the in vitro generation of Tregs (Fig. 4*F*). In IL-6– and IL-23–induced Th17 development, STAT3 activation is a critical step (19, 20). We found that STAT3 phosphorylation in CD4$^+$ T cells, in response to either IL-6 or IL-23, was severely impaired in cells with antagomir against miR-301a (Fig. 4*G*). In addition to STAT3 phosphorylation, IL-6 activation also results in signaling from two other pathways: STAT1 and PI3K/AKT (21, 22). However, we found that both STAT1 and AKT phosphorylation in CD4$^+$ T cells, after IL-6 stimulation, was unaffected by transfection of antagomir to miR-301a (Fig. 4*G*). These results suggest an association between miR-301a and IL-6 function in Th17 differentiation.

To exclude a direct effect of miR-301a on IL-6 receptors or STAT3 levels, we assessed expression of these genes in CD4$^+$ T cells transfected with antagomir to miR-301a. We found no changes in IL-6 receptor alpha (*Il6rα*), IL-6 signal transducer

(*Il6st*; gp130) or *Stat3* message levels in T-helper cells following inhibition of miR-301a (Fig. 4*H*). Thus, it appears that miR-301a inhibition impairs IL-6–induced signaling by selective interaction with events leading to STAT3 activation.

miR-301a Interferes with Intracellular Levels of PIAS3. We next searched bioinformatic databases (MIRANDA, PicTar, and TargetScan) to identify possible miR-301a target molecules in the IL-6–STAT3 pathway. We also analyzed four recently reported potential targets of miR-301a, *Nkrf* (23), *FoxF2*, *Bbc3*, and *Pten* (24). Of these 13 tested putative target genes, the major increase following miR-301a inhibition was found for *Pias3* (Fig. 5*A*). The miRNA target-prediction software RNAhybrid (version 2.1; http://bibiserv.techfak.uni-bielefeld.de/rnahybrid/) in concert with a MIRANDA search revealed the presence of two major binding sites for miR-301a within the *Pias3* RNA 3′UTR (Fig. 5*B*). Thus, *Pias3* RNA represents an attractive target for the action of miR-301a. To confirm a link between miR-301a and PIAS3, we transfected $CD4^+$ T cells with miR-301a mimics or antagomirs and analyzed the levels of PIAS3 (Fig. 5*C*). PIAS3 levels clearly were diminished in cells treated with miR-301a mimics and were increased in cells with an miR-301a inhibitor. In contrast, mimics or antagomirs for miR-21 and miR-155 had no effect on PIAS3 levels (Fig. 5*C*).

Next, using a luciferase reporter system, we sought to confirm that miR-301a directly binds the mRNA encoding Pias3 and down-regulates expression of this protein. HEK-293 cells were transfected with a construct containing the full-length Pias3 3′ UTR sequence downstream of firefly luciferase. The transfected cells showed luciferase activity, which the cotransfection with miR-301a inhibited by 82% (Fig. 5*D*). Neither transfection of control oligonucleotide into the cells expressing Pias3 3′ UTR-modified luciferase nor transfection of an miR-301a mimic into the cells with a wild-type luciferase affected the luciferase activity. These data confirm that miR-301a directly targets the mRNA encoding Pias3 and reduces expression of this protein.

Because our data showed differential expression of miR-301a in different T-helper subsets (Fig. 4*A*), we analyzed the expression of *Pias3* in the same T-helper populations (Fig. 5*E*). We found the *Pias3* transcript to be nearly absent in Th17 cells, in contrast to both Th1 and Th2 cells. This result supports the

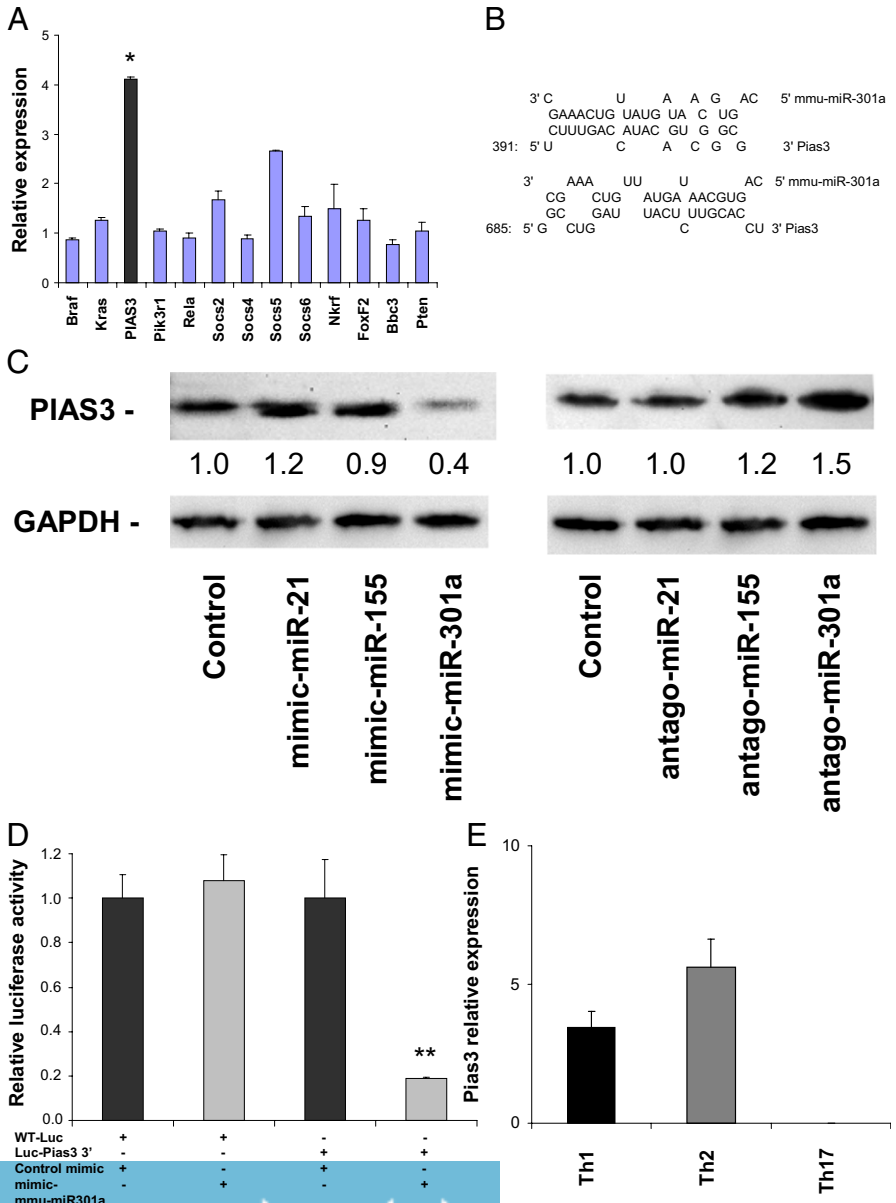

Fig. 5. miR-301a down-regulates PIAS3 in $CD4^+$ T cells. (*A*) $CD4^+$ T cells were transfected with antagomir against miR-301a or with a control antagomir and were stimulated in vitro with plate-bound anti-CD3 and anti-CD28 for 3 d. Antagomir-positive cells were sorted by flow cytometry. RNA was isolated and analyzed for the expression levels of *Braf*, *Kras*, *Pias3*, *Pik3r*, *Rela*, *Socs2*, *Socs4*, *Socs5*, *Socs6*, *Nkrf*, *FoxF2*, *Bbc3*, and *Pten* by qPCR. Data were normalized to the expression levels in $CD4^+$ T cells transfected with control antagomir. Representative results (mean ± SEM) from four independent experiments are shown. $*P < 0.01$. (*B*) Prediction of major interference sites between miR-301a and Pias3 mRNA 3′ UTR. (*C*) Western blot analysis of PIAS3 and GAPDH in $CD4^+$ T cells that were transfected with mimics against miR-21, miR-155, or miR-301a or with control oligonucleotide (*Left*) or with antagomirs for miR-21, miR-155, or miR-301a or with control oligonucleotide (*Right*) and were stimulated in vitro with plate-bound anti-CD3 and anti-CD28 for 3 d. Numerical values represent quantification by densitometry, normalized to the GAPDH levels and compared with the T cells transfected with the control oligonucleotide. Representative results from three independent experiments are shown. (*D*) Luciferase activity in HEK-293 cells transfected with reporter constructs containing either wild-type firefly luciferase or luciferase with Pias3 3′ UTR. The HEK-293 cell line was cotransfected with the indicated constructs and with either an miR-301a mimic or control oligonucleotide; normalized levels of luciferase activity are shown. Representative results (mean ± SEM) from two independent experiments are shown. $**P < 0.001$. (*E*) RNA was extracted from ex vivo sorted Th1, Th2, and Th17 cells and analyzed for expression levels of *Pias3* by qPCR. The data were normalized to the expression levels of naive $CD4^+$ T cells. Representative results (mean ± SEM) from two or three independent experiments are shown.

notion that the presence of miR-301a has a negative effect on *Pias3* expression in Th17 cells.

Modulation of miR-301a and PIAS3 Directly Changes in Vivo Encephalitogenicity of CD4$^+$ T Cells. To assess the in vivo relevance of miR-301a in myelin-specific CD4$^+$ T cells for the development of autoimmune demyelination, we used a transfer model of EAE in Rag2-KO mice. 2D2 T cells were transfected with miR-301a mimic, miR-301a antagomir, or a control scrambled oligonucleotide and were grafted into Rag2-KO mice in which EAE subsequently was induced. Mice from all groups developed signs of disease with a similar day of onset (Fig. 6*A*). However, over the next 25 d of observation, the mice that received 2D2 CD4$^+$ T cells expressing a mimic of miR-301a developed a very aggressive form of EAE that resulted in the death of all tested animals. In contrast, the group that received 2D2 CD4$^+$ T cells with an antagomir for miR-301a developed a significantly milder EAE (Fig. 6*A*). EAE in these mice also was less severe than in animals that received control transfected 2D2 CD4$^+$ T cells. We recovered infiltrating CD4$^+$ T cells from the CNS of Rag2-KO mice that had received 2D2 T cells that were transfected with either mimic, or antagomir-miR-301a or with a control oligonucleotide. Using fluorescein-labeled oligonucleotides for transfection, we were able to detect a significant fraction of fluorescein-positive CD4$^+$ T cells in the CNS of these mice as late as 15 d after transfer (Fig. 6*B*). In accordance with the clinical data, the mice that received the mimic miR-301a–transfected 2D2 T cells had an increased number of CD4$^+$ T-cells in their CNS at 15 d after transfer, whereas mice that received 2D2 T cells with antagomir miR-301a had significantly smaller infiltrates (Fig. 6*C*). Furthermore CD4$^+$ T cells in the CNS of mice that received 2D2 T cells with antagomir miR-301a produced less IL-17, whereas CD4$^+$ T cells in the CNS of mice that received 2D2 T cells with mimic miR-301a had increased IL-17 generation (Fig. 6*D*).

Because PIAS3 appeared to be an important intermediary of miR-301a in CD4$^+$ T cells, we also tested the effect of PIAS3 inhibition on EAE development. We inhibited PIAS3 in 2D2 CD4$^+$ T cells using a combination of three different siRNAs to enhance the knockdown effect (Fig. 6*E*). The transfer of such cells into Rag2-KO mice resulted in severe, fatal EAE in all animals (Fig. 6*F*), thus resembling the disease profile induced by transfer of $MOG_{35–55}$-specific CD4$^+$ T cells with up-regulated miR-301a (Fig. 6*A*). Taken together, these in vivo results confirmed the role of miR-301a and its target molecule, PIAS3, in the regulation of EAE.

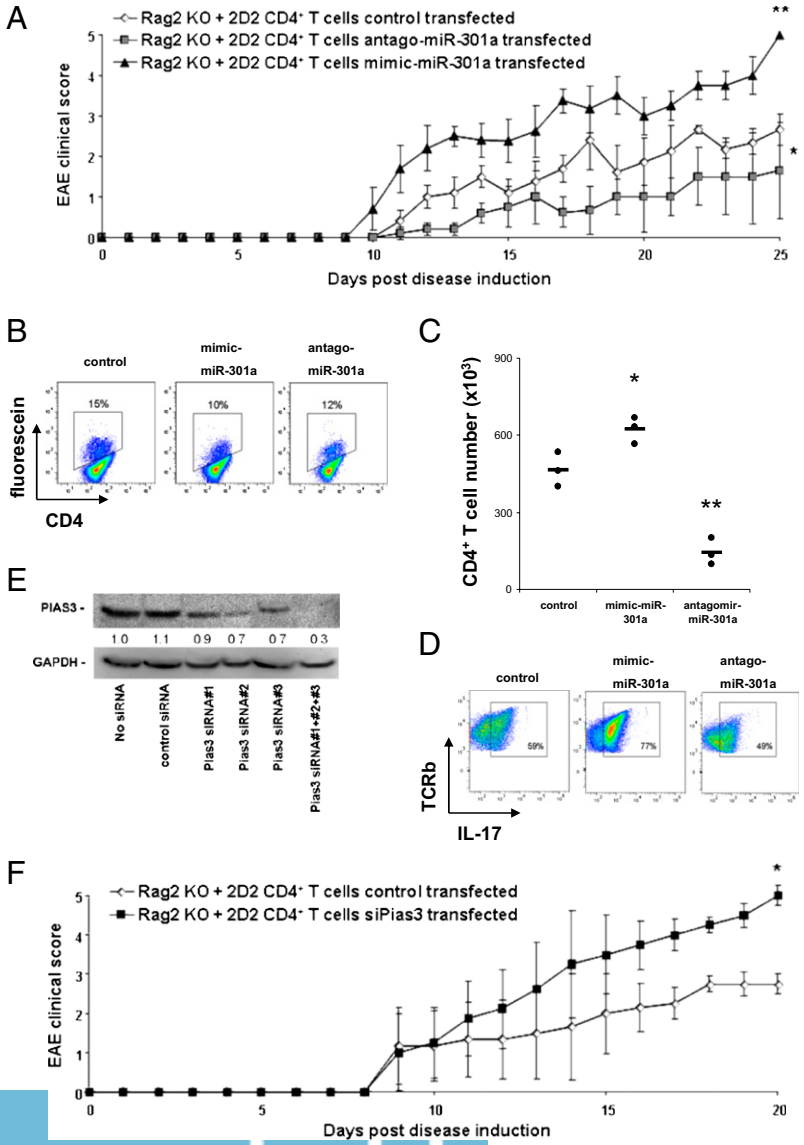

Fig. 6. Analysis of in vivo function of miR-301a and PIAS3 in myelin-specific CD4$^+$ T cells in EAE development. (*A*) 2D2 cells were isolated and transfected in vitro with antagomir against miR-301a or with a mimic for miR-301a or with a control oligonucleotide and were transferred to Rag2-KO mice in which EAE with $MOG_{35–55}$ subsequently was induced. Clinical scores of the mice are presented as mean ± SEM. Scoring is described in *Materials and Methods*. Five mice per group were used. *$P < 0.03$, **$P < 0.02$. (*B*) The percentage of the fluorescein-positive CNS-infiltrating CD4$^+$ T cells in Rag2-KO mice described in *A* was determined by flow cytometry analysis of gated CD4$^+$ T cells at 15 d after transfer. Representative results from three different mice per group are shown. (*C*) Quantification of CNS-infiltrating CD4$^+$ T cells in Rag2-KO mice described in *A* at 15 d after transfer. Each dot represents an individual mouse brain; horizontal lines mark the mean. *$P < 0.03$, **$P < 0.02$. (*D*) The intracellular production of IL-17 by CNS-infiltrating CD4$^+$ T cells in Rag2-KO mice described in *A* was determined by flow cytometry analysis of gated CD4$^+$ T cells at 15 d after transfer. Representative results from three different mice per group are shown. (*E*) Western blot analysis of PIAS3 and GAPDH in CD4$^+$ T cells 3 d after transfection with three different siRNAs for Pias3, alone or combined, or with control siRNA and in untransfected T cells. Numerical values represent quantification by densitometry, normalized according to the GAPDH levels and compared with the untransfected condition. Representative results from three independent experiments are shown. (*F*) 2D2 cells were isolated and transfected in vitro with a mixture of three of the siRNAs against Pias3 (described above) or with a control siRNA and then were transferred to Rag2-KO mice in which EAE with $MOG_{35–55}$ subsequently was induced. Clinical scores of the mice (described in *Materials and Methods*) are presented as mean ± SEM. Five mice per group were used. *$P < 0.03$.

Discussion

Our findings indicate that the development of myelin antigen-specific $CD4^+$ T cell responses correlates with significant changes in miRNA expression profiles in peripheral and brain-infiltrating T cells. The most notable up-regulations were observed for miR-301a, miR-21, and miR-155. Mechanistic studies showed that miR-301a influenced the development of Th17 cells via inhibition of the IL-6–induced STAT3 pathway. A molecular search highlighted and validated PIAS3, a STAT3 inhibitor, as a target of miR-301a in $CD4^+$ T cells. In vivo studies in animals with EAE and manipulation of miR-301a levels in myelin-autoreactive $CD4^+$ T cells demonstrated a specific role for miR-301a in the regulation of EAE. Accordingly, inhibition of PIAS3, a target molecule for miR-301a, resulted in up-regulation of EAE. Thus, we have confirmed a significant role for miRNA in the regulation of autoimmune demyelination and have demonstrated a specific role of miR-301a and its target molecule PIAS3 as critical players in this process.

Many observations link changes in miRNA expression to the development of autoimmunity. For example, general ablation of miRNA in T cells by conditional deletion of Dicer resulted in the spontaneous development of autoimmunity in aged mice (25). This phenomenon has been linked in particular to the loss of function of miRNA-deficient Tregs, and mice with either a general deficiency of miRNA or selective knockdown of miR-146a in Tregs displayed a fatal autoimmune disease (26–30). However, miRNA ablation in T cells also results in defects in natural killer T-cell development (31, 32) and the differentiation of T-helper cells that may contribute independently to autoimmunity (25, 33).

miR-301a, a highly evolutionarily conserved miRNA, along with miR-130a, miR-130b, and miR-301b, belongs to the miR-130/301 family in the mouse genome (www.mirbase.org; ref. 34). Recently, Mir-301a has been reported as being expressed in response to activation in $CD8^+$ T cells, where it probably plays a role as a regulator of CD69 expression (35). miR-301a also has been identified among the miRNA enriched in Th1 and Th2 populations (36). Additionally miR-301a is up-regulated in response to IL-6 stimulation of malignant cholangiocytes (37). We found miR-301a to be significantly and specifically up-regulated in $CD4^+$ T cells during myelin antigen recognition. miR-301a also is strongly up-regulated within CNS T cells in animals with EAE, where its up-regulation was found to be monophasic and related to the clinically acute period of the disease. Although miR-301a appeared to be up-regulated following TCR stimulation, the inhibition of miR-301a did not influence the proliferative responses of the $CD4^+$ T cells. Most significantly, miR-301a inhibition down-regulated secretion of IL-17 and expression of the Th17 population marker genes such as *Rora*, *Rorc-γt*, and *Ahr*. miR-301a expression was particularly pronounced in Th17 cells, both in vivo and in vitro, suggesting that miR-301a modulates Th17 development. Indeed, miR-301a blockade in vitro hampered the generation of Th17 cells but had no effect on the capacity to generate Tregs. Most intriguingly, signaling of IL-6 and IL-23 was blocked substantially by down-regulation of miR-301a with a specific antagomir, leading to marked loss of STAT3 phosphorylation but not of STAT1 or AKT activation. The activation of the IL-6/23–induced STAT3 pathway is a critical and specific step required for the generation and maintenance of Th17 cells (19, 20). Thus, miR-301a directly affects Th17 cell development.

A subsequent search for a molecular mechanism for the action of miR-301a on Th17 cell development demonstrated that interference with PIAS3 is likely to mediate this effect. PIAS3 is an E3 SUMO ligase that has been shown to act as both a transcriptional coactivator and a corepressor and to regulate the activity of many classes of transcription factors (38). However, PIAS3 activity has been linked primarily to the inhibition of STAT3 (39). So far little has been known about the role of PIAS3 in T-helper cell differentiation and function and in particular in the control of Th17 generation. In this study we have demonstrated that, although the PIAS3 transcript is essentially absent in Th17 cells, it is readily detectable in both the Th1 and Th2 subsets. Furthermore, a transfer of myelin-specific $CD4^+$ T cells with siRNA-mediated knockdown of PIAS3 resulted in severely up-regulated EAE in recipient animals. Thus, PIAS3 inhibition alone was sufficient to mimic the effect of miR-301a up-regulation. This observation indicates an inverse relationship between miR-301a and PIAS3 and functionally supports the notion that miR-301a down-regulates PIAS3, promoting Th17 development. Thus, we suggest here a role for PIAS3 as a regulator of Th17 subset development and function. In this regard, it is interesting that a related E3 SUMO ligase, PIAS1, recently has been demonstrated to be a critical factor involved in the regulation and accessibility of the Foxp3 locus influencing Treg development, also with strong implications for the pathogenesis of EAE (40).

Our miRNA profiling of $CD4^+$ T cells responding to $MOG_{35–55}$ identified, in addition to miR-301a, up-regulation of two other miRNAs, miR-21 and miR-155. Mir-155 was among the first miRNAs identified as operating in T cells, and its expression has been linked to activation following TCR stimulation (41, 42). Mice deficient in miR-155 develop an increased inflammatory remodeling of lung airways, reminiscent of autoimmune-mediated lung fibrosis and enteric inflammation (16). The underlying deficit leading to autoimmunity in these mice has been associated with overproduction of Th2 cells caused by an imbalance of T-cell subset differentiation. In our study, we also noted an up-regulation of the Th2 marker gene, *Gata3*, following inhibition of miR-155 in T cells. We also found a marked up-regulation of miR-155 in T-helper cells during the development of autoimmune demyelination, both in lymphocytes in the periphery and in brain-infiltrating cells. Indeed, it has been demonstrated recently that miR-155–deficient mice are significantly resistant to EAE induction (11). This resistance has been related largely to the $CD4^+$ T-cell–intrinsic function of miR-155, and our findings support this notion. Additionally, elevated expression of miR-155 has been observed in brain lesions from MS patients (43). miR-155 has been shown to be important for many other immune cell populations, e.g., for Ig class switching to IgG in B cells (16, 44–46) and for the function and development of myeloid cells, particularly in the context of LPS responses (47–49). Notably, miR-155 deficiency affects dendritic cell function during EAE, contributing to the observed EAE resistance phenotype (11). Thus, the final outcome of miR-155 activity in EAE may depend on several factors.

Another miRNA that we noted as being significantly associated with myelin-autoreactive $CD4^+$ T-cell responses is miR-21. miR-21 previously has been demonstrated to be overexpressed in MS lesions (43). A number of reports link miR-21 and T-cell function. miR-21 was found to be highly represented in effector and memory T cells compared with naive $CD8^+$ T cells (50). In human Tregs, miR-21 was found to act as a positive, although indirect, regulator of FOXP3 expression (51). Furthermore, miR-21 was found to be overexpressed in $CD4^+$ T cells derived both from patients with lupus and from lupus-prone MRL/lpr mice (52). Most notably, miR-21 has been described as an "oncomiR," meaning that it is overexpressed in most tumor types analyzed so far and is involved functionally in oncogenic processes (53, 54). Although the changes in miR-21 expression that we observed during EAE suggest a role for this miRNA in autoimmune demyelination, we have not observed any significant changes in T-cell function following miR-21 inhibition. Thus, the role of miR-21 in autoimmune demyelination will require further studies.

In summary, our findings demonstrate the role of miR-301a and its putative target, PIAS3, in the development of Th17 cells and thus in the regulation of EAE. Recently, accumulating data strongly suggest that Th17 cells represent a plastic and probably transient population of T-helper cells. Such a scenario would require the ability to repress and restore quickly the transcription of lineage master controlling genes. miRNA, including miR-301a, would be ideally suited to perform such an action. Indeed, the effect of miR-301a up-regulation in EAE was mimicked by

the effect of siRNA-mediated knockdown of PIAS3 in myelin-reactive CD4$^+$ T cells. Collectively, our results suggest that miR-301a is a Th17 subset-associated miRNA that functions in the pathogenesis of autoimmune demyelination and might represent an important target for potential therapeutic intervention.

Materials and Methods

Mice. C57BL/6 mice were purchased from Jackson Laboratories; Rag 2-KO mice were purchased from Taconic; and MOG-TCR transgenic 2D2 mice were obtained from T. Ovens (University of Southern Denmark, Odense, Denmark). Mice were maintained in our colony for the experiments. All animal protocols were approved by the Institutional Animal Care and Use Committee of the Medical University of Lodz.

Antibodies, Cytokines, and Peptides. The fluorochrome-conjugated antibodies specific for CD3, CD4, CD11b, CD19, CD25, CD45, FOXP3, IL-17, IFN-γ, phosphorylated STAT1 (pSTAT1; pY701), phosphorylated STAT3 (pSTAT3; pY705), and phosphorylated AKT (pAKT; pT308) were purchased from BD Biosciences. Antibody to PIAS3 was purchased from Sigma, and antibody to GAPDH was purchased from Santa Cruz. $MOG_{35–55}$ peptide was purchased from Peptide 2.0. IL-6 and IL-2 were purchased from Peprotech; IL-1β was purchased from Sigma; TGF-β and IL-23 were purchased from R&D Systems.

Immunization and T-Cell Cultures and Assays. C57BL/6 mice (8–12 wk old) were immunized s.c. over the abdominal flanks of with 0.15 mg $MOG_{35–55}$ peptide in 150 μL CFA (Sigma) containing 0.75 mg *Mycobacterium tuberculosis* (Difco Laboratories). PLN (both popliteal and inguinal nodes) were isolated, and single-cell suspensions were cultured in triplicate at a density of 2×10^5 cells per well in 200-uL U-bottomed microtiter well plates. For 2D2 T-cell responses analogous cultures were set up from PLN of 8- to 12-wk-old unimmunized $MOG_{35–55}$-TCR transgenic 2D2 mice. To detect protein expression of IL-4, IL-10, IL-17, and IFN-γ, ELISAs were performed in supernatants of 72-h cultures using cytokine-specific kits from R&D Systems and carried out according to the manufacturer's instructions. For RNA isolation, cultured CD4$^+$ T cells were isolated by indirect magnetic sorting with the CD4$^+$ T Cell Isolation Kit II (Miltenyi Biotech). To assay the proliferation, after 72-h culture, 3H-labeled thymidine (TdR; Amersham) (1 uCi per well) was added for the final 18 h of culture, and uptake was measured using a liquid scintillation beta counter (PerkinElmer). Results were expressed as cpm.

CD4$^+$ T-Cell Subpopulations, ex Vivo Isolation, and in Vitro Differentiation. To obtain the Th1, Th2, and Th17 ex vivo populations, single-cell cultures of splenocytes of C57BL/6 mice were stimulated overnight with phorbol dibutyrate (500 ng/mL) and ionomycin (1,000 ng/mL) followed by the magnetic enrichment of cytokine-secreting cells with kits from Miltenyi Biotech according to the manufacturer's instructions. Th1 cells were enriched for IFN-γ secretion, Th2 cells for IL-4 secretion, and Th17 cells for IL-17 secretion. Finally, high-purity ex vivo subpopulations were obtained by flow cytometry sorting of the six color-stained cytokine-enriched fractions. In vitro differentiation of Th17 cells was performed by magnetic sorting of naive splenic CD4$^+$ T cells from C57BL/6 mice with the CD4$^+$ CD62L$^+$ T Cell Isolation Kit II (Miltenyi Biotech) and subsequent culture in Iscove's modified Dulbecco's medium (IMDM) supplemented with IL-6 (25 ng/mL), TGF-β (2 ng/mL), IL-1β (20 ng/mL), and IL-23 (20 ng/mL), under stimulation by plate-bound anti-CD3 (145–2C11; 5 μg/mL) and anti-CD28 (37.51; 10 μg/mL) in the presence of anti–IL-4 (11B11; 10 μg/mL) and anti–IFN-γ (XMG1.2; 10 μg/mL). In vivo differentiation of Th0, Th1, and Th2 cells and Tregs was performed by magnetic sorting of naive splenic CD4$^+$ T cells from C57BL/6 mice using the CD4$^+$ CD62L$^+$ T Cell Isolation Kit II (Miltenyi Biotech) and subsequent culture in IMDM supplemented with anti–IL-4 (11B11; 10 μg/mL) and anti–IFN-γ (XMG1.2; 10 μg/mL) for Th0 cells; with IL-12 (10 ng/mL) in the presence of anti–IL-4 (11B11; 10 μg/mL) and anti–IFN-γ (XMG1.2; 10 μg/mL) for Th1 cells; with IL-4 (40 ng/mL) in the presence of anti–IFN-γ (XMG1.2; 10 μg/mL) for Th2 cells; or with TGF-β (10 ng/mL) and IL-2 (100 U/mL) in the presence of anti–IL-4 (11B11; 10 μg/mL) and anti–IFN-γ (XMG1.2; 10 μg/mL) for Tregs under stimulation by plate-bound anti-CD3 (145–2C; 115 μg/mL) and anti-CD28 (37.51; 10 μg/mL).

Isolation of Brain Mononuclear Cells. Mice were perfused intracardially with PBS before the dissection of the brain, which subsequently was homogenized. Brain mononuclear cells were isolated using 37–70% (vol/vol) Percoll gradients.

Transfections of Antagomirs Against miR-21, mir-155, mir-301a, Mimics for miR-21, miR-155, miR-301a, and siRNA for Pias3. Antagomirs against miR-21, miR-155, and miR-301a labeled with 5′-fluorescein and control antagomir (scrambled oligonucleotide) labeled with 5′-fluorescein were purchased from Exiqon Inc. Mimics for miR-21, mir-155, and mir-301a and control mimic (scrambled oligonucleotide) were purchased from Thermo Scientific. siRNAs for Pias3 (#1: s202481; #2: s202482; #3: s106248) and control siRNA were purchased from Applied Biosystems. Oligonucleotides were complexed with Lipofectamine 2000 (Invitrogen Life Technologies) according to the manufacturer's instructions. Briefly, oligonucleotides were incubated first with X-VIVO 15 medium (Lonza) for 5 min at room temperature and subsequently with Lipofectamine 2000 (Invitrogen Life Technologies) for 20 min at room temperature and then were added to either the PLN or the T-cell culture in 24-well plates at a final concentration of 180 nM for overnight transfection at 37 °C. On the following day, T cells were harvested, washed with PBS, and used for subsequent assays. The effectiveness of the transfection was monitored by presence of the fluorescein-positive cells in flow cytometry analyses.

Extraction of RNA, Analysis of miRNA, and mRNA Expression. RNA was extracted using a mirVana kit (Ambion). RNA isolated from a small number (<100,000) of cells sorted by flow cytometry was amplified using a TransPlex Complete Whole Transcriptome Amplification Kit (Sigma) according to the manufacturer's instructions. For quantitative analysis of RNA expression, we carried out real-time quantitative RT-PCR (qRT-PCR) using TaqMan (Applied Biosystems). The miRNA expression data were normalized for the expression of U6 snRNA, and the mRNA expression data were normalized for the expression of TATA-binding protein. Quantitative analysis of Ror-γt expression was performed using Power SYBR Green PCR Master Mix (Applied Biosystems). Relative levels of Ror-γt expression were determined using GAPDH as the control. The sequences of the primers used were Ror-γt-F, 5′-CCGCTGAGAGGGCTTCAC; Ror-γt-R, 5′-TGCAGGAGTAGGCCACATTACA; GAPDH-F, 5′-AGTATGACTCCACTCACGGCAA; GAPDH-R, 5′-TCTCGCTCCTGGAAGATGGT. Microarray analysis of miRNA expression was performed at Exiqon Inc. using a miRCURY LNA Array, version 10.0. All array data have been deposited in the Gene Expression Omnibus (GEO) database (http://www.ncbi.nlm.nih.gov/geo/), accession no. GSE28473.

Luciferase Reporter Assay for Target Validation. HEK-293 cells were transfected with pEZX-MT01 vectors containing wild-type firefly luciferase or firefly luciferase with PIAS3 3′ UTR (GeneCopoeia) and with 50 nM of mimic miR-301a or negative-control oligonucleotide (Thermo Scientific). The cells were lysed, and luciferase activity was measured 24 h after transfection using Victor ×4 (Perkin-Elmer).

Flow Cytometry and Cell Sorting. We performed one- to six-color flow cytometry analysis with LSR II equipment (Beckton Dickinson) according to standard procedures. For intracellular detection of cytokine production, T cells were stimulated with 500 ng/mL phorbol dibutyrate and 500 ng/mL ionomycin in the presence of brefeldin A for 6 h. Detection of IL-17–, IFN-γ–, or FOXP3-positive CD4$^+$ T cells was performed by intracellular staining using a Mouse Regulatory T-cell Staining Kit (eBioscience), according to the manufacturer's instructions. pSTAT1 (pY701), pSTAT3 (pY705), and pAKT (pT308) were detected by intracellular staining using a Phosphoflow Perm Buffer III (BD Biosciences), according to the manufacturer's instructions. Cell sorting was performed following a four- to six-color flow cytometry analysis with BD Aria equipment (Beckton Dickinson) according to standard procedures.

Induction of EAE. We induced active EAE by s.c. immunization over the abdominal flanks of 8- to 12-wk-old C57BL/6 mice with 0.15 mg $MOG_{35–55}$ peptide in 150 μL CFA (Sigma) containing 0.75 mg *M. tuberculosis* (Difco Laboratories). In addition, 0.2 μg Pertussis toxin (Sigma) was injected into a tail vein on days 0 and 2. Mice were observed daily for neurologic signs of EAE and were scored on a numerical scale from 0–5 as follows: 0, no disease; 1, weak tail or wobbly walk; 2, hind limb paresis; 3, hind limb paralysis; 4, hind and forelimb paralysis; 5, death or euthanasia for humane reasons.

Transfer Model of EAE in the Rag2-KO Mice. The 2D2 cells were isolated from PLN and spleens of unimmunized 2D2 mice and were transfected in vitro with antagomir against miR-301a or with a mimic for miR-301a or with a control oligonucleotide as described above. After 24 h of culture, 2D2 transgenic CD4$^+$ T cells were washed, and 2×10^6 cells were transferred i.v. into naive 10-wk-old Rag2-KO female mice. Active EAE was induced on the day CD4$^+$ T cells were transferred. Mice were observed daily for neurologic signs of EAE and were scored as described above.

Western Blot Analysis. The cells were lysed, and total cell lysates were resolved on SDS electrophoresis gels by standard procedures. Immunoblotting was performed with mouse primary antibodies to PIAS3 (Sigma) and GAPDH (Santa Cruz) and was visualized by ChemiImager (Alpha Innotech). Quantitative densitometry analysis was performed using the program AlphaEaseFC (Alpha Innotech).

Statistical Analysis. Results were compared using the program StatGraphics Centurion XV (StatPoint Technologies). The clinical data from groups of mice with EAE were compared using the Mann–Whitney *u* test. Proliferation, cytokine secretion, and qPCR and flow cytometry data were compared using the Student's *t* test. *P* values <0.05 were considered statistically significant.

ACKNOWLEDGMENTS. The 2D2 mice were kindly provided by T. Owens (Department of Neurobiology Research, University of Southern Denmark) through European Cooperation in Science and Technology (COST) BM0603. We thank D. Bending (Department of Pathology, University of Cambridge) for the help with the in vitro Th17 differentiation protocol and C. F. Brosnan (Albert Einstein College of Medicine) for discussion and editing of our manuscript. This work was supported by Polish Ministry of Science Grants 194/N-COST/2008/0, COST BM0603, and 0460/B/P01/2009/36 and by Polpharma Science Foundation Grant 13/IV/2005 (all to K.W.S.); by a European Research Area Network (ERA.Net) RUS/388/2012 (to M.P.M.); and by Polish National Science Center Grant 2011/01/N/NZ6/01849 (to M.C.). A.M. was supported within the Action 2.6 of the Integrated Operational Program of the Regional Development of the European Social Fund.

1. Sospedra M, Martin R (2005) Immunology of multiple sclerosis. *Annu Rev Immunol* 23: 683–747.
2. Hafler DA (2004) Multiple sclerosis. *J Clin Invest* 113:788–794.
3. Bettelli E, Korn T, Oukka M, Kuchroo VK (2008) Induction and effector functions of T(H)17 cells. *Nature* 453:1051–1057.
4. Eugster HP, Frei K, Kopf M, Lassmann H, Fontana A (1998) IL-6-deficient mice resist myelin oligodendrocyte glycoprotein-induced autoimmune encephalomyelitis. *Eur J Immunol* 28:2178–2187.
5. Bettelli E, et al. (2006) Reciprocal developmental pathways for the generation of pathogenic effector TH17 and regulatory T cells. *Nature* 441:235–238.
6. Cua DJ, et al. (2003) Interleukin-23 rather than interleukin-12 is the critical cytokine for autoimmune inflammation of the brain. *Nature* 421:744–748.
7. Xiao C, Rajewsky K (2009) MicroRNA control in the immune system: Basic principles. *Cell* 136:26–36.
8. Jinek M, Doudna JA (2009) A three-dimensional view of the molecular machinery of RNA interference. *Nature* 457:405–412.
9. Selbach M, et al. (2008) Widespread changes in protein synthesis induced by microRNAs. *Nature* 455:58–63.
10. Du C, et al. (2009) MicroRNA miR-326 regulates TH-17 differentiation and is associated with the pathogenesis of multiple sclerosis. *Nat Immunol* 10:1252–1259.
11. O'Connell RM, et al. (2010) MicroRNA-155 promotes autoimmune inflammation by enhancing inflammatory T cell development. *Immunity* 33:607–619.
12. Ponomarev ED, Veremeyko T, Barteneva N, Krichevsky AM, Weiner HL (2011) MicroRNA-124 promotes microglia quiescence and suppresses EAE by deactivating macrophages via the C/EBP-alpha-PU.1 pathway. *Nat Med* 17(1):64–70.
13. Krützfeldt J, et al. (2005) Silencing of microRNAs in vivo with 'antagomirs'. *Nature* 438:685–689.
14. Krützfeldt J, et al. (2007) Specificity, duplex degradation and subcellular localization of antagomirs. *Nucleic Acids Res* 35:2885–2892.
15. Bettelli E, et al. (2003) Myelin oligodendrocyte glycoprotein-specific T cell receptor transgenic mice develop spontaneous autoimmune optic neuritis. *J Exp Med* 197: 1073–1081.
16. Rodriguez A, et al. (2007) Requirement of bic/microRNA-155 for normal immune function. *Science* 316:608–611.
17. Reboldi A, et al. (2009) C-C chemokine receptor 6-regulated entry of TH-17 cells into the CNS through the choroid plexus is required for the initiation of EAE. *Nat Immunol* 10:514–523.
18. Korn T, Bettelli E, Oukka M, Kuchroo VK (2009) IL-17 and Th17 Cells. *Annu Rev Immunol* 27:485–517.
19. Yang XO, et al. (2007) STAT3 regulates cytokine-mediated generation of inflammatory helper T cells. *J Biol Chem* 282:9358–9363.
20. Zhou L, et al. (2007) IL-6 programs T(H)-17 cell differentiation by promoting sequential engagement of the IL-21 and IL-23 pathways. *Nat Immunol* 8:967–974.
21. Chen RH, Chang MC, Su YH, Tsai YT, Kuo ML (1999) Interleukin-6 inhibits transforming growth factor-beta-induced apoptosis through the phosphatidylinositol 3-kinase/Akt and signal transducers and activators of transcription 3 pathways. *J Biol Chem* 274:23013–23019.
22. Heinrich PC, Behrmann I, Müller-Newen G, Schaper F, Graeve L (1998) Interleukin-6-type cytokine signalling through the gp130/Jak/STAT pathway. *Biochem J* 334: 297–314.
23. Lu Z, et al. (2011) miR-301a as an NF-κB activator in pancreatic cancer cells. *EMBO J* 30: 57–67.
24. Shi W, et al. (2011) MicroRNA-301 mediates proliferation and invasion in human breast cancer. *Cancer Res* 71:2926–2937.
25. Cobb BS, et al. (2005) T cell lineage choice and differentiation in the absence of the RNase III enzyme Dicer. *J Exp Med* 201:1367–1373.
26. Lu LF, et al. (2010) Function of miR-146a in controlling Treg cell-mediated regulation of Th1 responses. *Cell* 142:914–929.
27. Cobb BS, et al. (2006) A role for Dicer in immune regulation. *J Exp Med* 203: 2519–2527.
28. Liston A, Lu LF, O'Carroll D, Tarakhovsky A, Rudensky AY (2008) Dicer-dependent microRNA pathway safeguards regulatory T cell function. *J Exp Med* 205:1993–2004.
29. Chong MM, Rasmussen JP, Rudensky AY, Littman DR (2008) The RNAseIII enzyme Drosha is critical in T cells for preventing lethal inflammatory disease. *J Exp Med* 205: 2005–2017.
30. Zhou X, et al. (2008) Selective miRNA disruption in T reg cells leads to uncontrolled autoimmunity. *J Exp Med* 205:1983–1991.
31. Zhou L, et al. (2009) Tie2cre-induced inactivation of the miRNA-processing enzyme Dicer disrupts invariant NKT cell development. *Proc Natl Acad Sci USA* 106: 10266–10271.
32. Fedeli M, et al. (2009) Dicer-dependent microRNA pathway controls invariant NKT cell development. *J Immunol* 183:2506–2512.
33. Muljo SA, et al. (2005) Aberrant T cell differentiation in the absence of Dicer. *J Exp Med* 202:261–269.
34. Griffiths-Jones S, Saini HK, van Dongen S, Enright AJ (2008) miRBase: Tools for microRNA genomics. *Nucleic Acids Res* 36(Database issue):D154–D158.
35. Zhang N, Bevan MJ (2010) Dicer controls CD8+ T-cell activation, migration, and survival. *Proc Natl Acad Sci USA* 107:21629–21634.
36. Kuchen S, et al. (2010) Regulation of microRNA expression and abundance during lymphopoiesis. *Immunity* 32:828–839.
37. Braconi C, Huang N, Patel T (2010) MicroRNA-dependent regulation of DNA methyltransferase-1 and tumor suppressor gene expression by interleukin-6 in human malignant cholangiocytes. *Hepatology* 51:881–890.
38. Yagil Z, et al. (2010) The enigma of the role of protein inhibitor of activated STAT3 (PIAS3) in the immune response. *Trends Immunol* 31:199–204.
39. Chung CD, et al. (1997) Specific inhibition of Stat3 signal transduction by PIAS3. *Science* 278:1803–1805.
40. Liu B, Tahk S, Yee KM, Fan G, Shuai K (2010) The ligase PIAS1 restricts natural regulatory T cell differentiation by epigenetic repression. *Science* 330:521–525.
41. Haasch D, et al. (2002) T cell activation induces a noncoding RNA transcript sensitive to inhibition by immunosuppressant drugs and encoded by the proto-oncogene, BIC. *Cell Immunol* 217:78–86.
42. Jindra PT, Bagley J, Godwin JG, Iacomini J (2010) Costimulation-dependent expression of microRNA-214 increases the ability of T cells to proliferate by targeting Pten. *J Immunol* 185:990–997.
43. Junker A, et al. (2009) MicroRNA profiling of multiple sclerosis lesions identifies modulators of the regulatory protein CD47. *Brain* 132:3342–3352.
44. Dorsett Y, et al. (2008) MicroRNA-155 suppresses activation-induced cytidine deaminase-mediated Myc-Igh translocation. *Immunity* 28:630–638.
45. Thai TH, et al. (2007) Regulation of the germinal center response by microRNA-155. *Science* 316:604–608.
46. Vigorito E, et al. (2007) microRNA-155 regulates the generation of immunoglobulin class-switched plasma cells. *Immunity* 27:847–859.
47. Tili E, et al. (2007) Modulation of miR-155 and miR-125b levels following lipopolysaccharide/TNF-alpha stimulation and their possible roles in regulating the response to endotoxin shock. *J Immunol* 179:5082–5089.
48. Androulidaki A, et al. (2009) The kinase Akt1 controls macrophage response to lipopolysaccharide by regulating microRNAs. *Immunity* 31:220–231.
49. O'Connell RM, Chaudhuri AA, Rao DS, Baltimore D (2009) Inositol phosphatase SHIP1 is a primary target of miR-155. *Proc Natl Acad Sci USA* 106:7113–7118.
50. Wu H, et al. (2007) miRNA profiling of naïve, effector and memory CD8 T cells. *PLoS ONE* 2:e1020.
51. Rouas R, et al. (2009) Human natural Treg microRNA signature: Role of microRNA-31 and microRNA-21 in FOXP3 expression. *Eur J Immunol* 39:1608–1618.
52. Pan W, et al. (2010) MicroRNA-21 and microRNA-148a contribute to DNA hypomethylation in lupus CD4+ T cells by directly and indirectly targeting DNA methyltransferase 1. *J Immunol* 184:6773–6781.
53. Volinia S, et al. (2006) A microRNA expression signature of human solid tumors defines cancer gene targets. *Proc Natl Acad Sci USA* 103:2257–2261.
54. Krichevsky AM, Gabriely G (2009) miR-21: A small multi-faceted RNA. *J Cell Mol Med* 13:39–53.